Research article

Low KeV virtual monoenergetic images for detecting low dose iodine- or alternative Gd-based IV contrast agents

Guang Li , Nikita Rednam , Vikas Kundra *

Department of Diagnostic Radiology and Nuclear Medicine, University of Maryland School of Medicine, 22 S. Greene St., Baltimore, MD, 21201, USA

ABSTRACT

Background: The recent shortage of iodine-based intravenous contrast and its cost highlight the need for limiting dose and alterative agents.

Purpose: To quantify radiodensity (Hounsfield Units, HU) improvement and potential iodine dose reduction with low keV imaging compared to conventional polyenergetic reconstructions on dual source (DSCT) and dual layer (DLCT) CT and to assess potential utility of non-iodine gadolinium-alternatives with low keV imaging.

Materials and methods: This phantom study used dilutions of three commercially-available contrast agents scanned by DSCT and DLCT. Conventional polyenergetic and virtual monoenergetic images (VMI) were reconstructed of each of five dilutions at five keV levels. HU and signal-to-noise ratios were compared among iodine- and gadolinium-based contrast agents.

Results: Iodine- and gadolinium-based contrast agent HU increased inversely to keV for the same dilution in both scanners. At the lowest keV setting (40 keV), iodine-based contrast agent HU in VMIs with DLCT and DSCT were approximately 300 % and 400 % of conventional, respectively. Gd-based contrast agent HU in VMIs at low keV were similar to or better than conventional iodine HU. Comparing the dual energy CTs, although HU from iodine and gadolinium-based contrast agents for conventional polyenergetic reconstructions was similar, HU in VMIs of DSCT were right shifted compared to DLCT by ~10 keV lower.

Conclusion: Depending on CT scanner type, 1/3 to 1/4 dose of iodinated contrast at 40 keV provides HU similar to full dose conventional acquisition, suggesting 1/3-1/4 dose may be adequate clinically at 40 keV. Depending on the Gd-based contrast and CT type, Gd-based contrast at 40 keV provides similar or greater HU compared to conventional acquisitions with iodinated contrast, suggesting Gd-based contrast at 40 keV may serve as an alternative to iodinated contrast. HU on VMI images is scanner dependent, suggesting scanner-dependent protocol optimization and potentially monoenergy HU calibration between scanners is needed.

1. Introduction

The recent shortage of iodine-based intravenous contrast has highlighted the need for limiting dose and searching for alterative intravenous (IV) contrast agents. Reducing iodinated IV contrast dose should enable significant cost savings and may reduce contrast-induced acute kidney injury [1]. The latter is especially relevant in patients with existing decreased kidney function [2,3] or with recent renal transplant [4]. Alternatives to iodinated contrast agents are those based on gadolinium [5], including those already clinically approved for MRI. Such agents have different levels of T1 relaxation for generating MR signal [6].

Conventional CT acquires projections at one mean-energy level while dual-energy CT (DECT) acquires two, enabling virtual monoenergetic reconstructions. Two methods are primarily used for DECT acquisitions. In the first, dual source CT (DSCT), x-ray beams at two different energy levels are generated by two x-ray sources and detected by two single-layer detectors. In the second, dual layer CT (DLCT), a single x-ray source is used and two different mean-energy levels are distinguished by a dual-layer detector. Virtual

---

monoenergetic images (VMI) are then generated. It has been suggested that 70 keV VMIs are similar to conventional polyenergetic images [7,8]. Theoretically, the amount of image contrast generated should increase as one approaches the k-edge of the molecule of interest and then decrease afterwards. The k-edge of iodine is 33 keV and Gd is 50 keV [9], suggesting radiodensity should theoretically increase to 33 keV for iodine and peak at 50 keV for Gd. It also suggests that the total amount of iodinated contrast may be reduced at lower keV to obtain similar Hounsfield units (HU) as conventional polyenergetic CT images. A few studies have used low keV and suggest improved lesion conspicuity using full iodinated contrast dose [10–18]. Studies investigating how different gadolinium-based agents perform in CT exams in comparison with iodine-based and whether different dual-energy CT techniques (i.e. DSCT vs. DLCT) affect HU on monoenergetic and polyenergetic reconstructions are lacking.
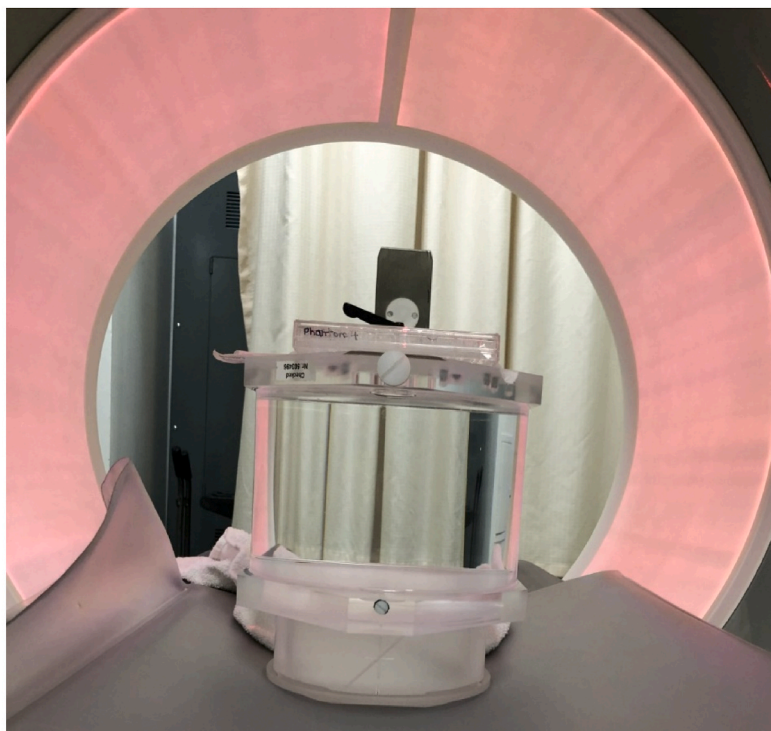
(a)
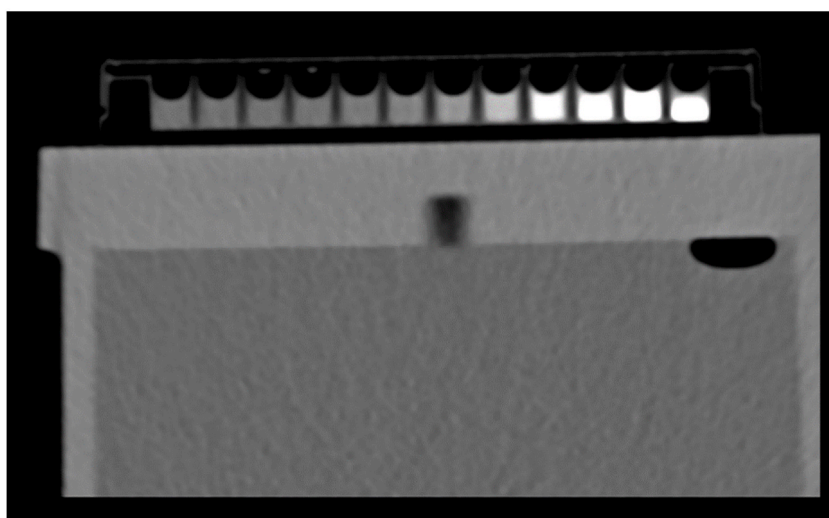
(b)

Fig. 1. a) The 96-well phantom on top of the water phantom in the CT gantry; b) axial CT images of the 96-well phantom on top of the water phantom.
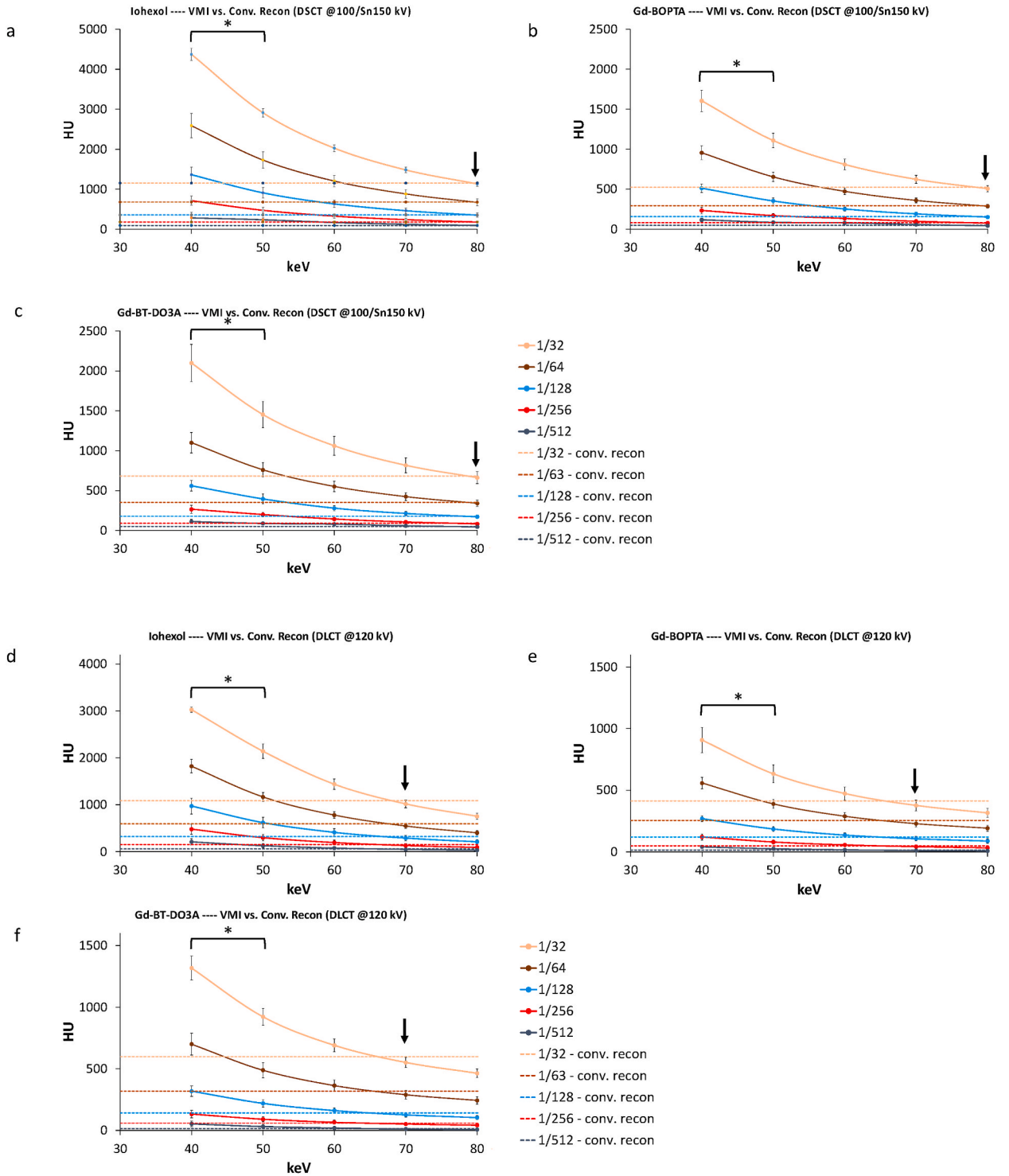
Fig. 2. HU by contrast agent concentration and keV. HU of iohexol, Gd-BOPTA and Gd-BT-DO3A versus keV at various concentrations on a dual source CT (a, b and c) and a dual-layer CT (d, e and f). Arrows points to where HU of monoenergetic reconstructions cross isobars indicating HU with conventional polyenergetic reconstruction. *, p < 00.05 in comparisons between 40 keV and 50 keV for iohexol, Gd-BOPTA and Gd-BT-DO3A. (DSCT: dual-source dual energy CT; DLCT: dual-layer dual energy CT).

We compared the radiodensity of various doses of iodinated contrast and two Gd contrast agents in two types of dual energy scanners, DSCT and DLCT. Our purpose was to quantify radiodensity (i.e. HU) improvement and potential iodine dose reduction with low keV imaging compared to conventional polyenergetic reconstruction on two different types of dual-energy CT scanners, and to assess the potential utility of non-iodine gadolinium-based alternatives with low keV imaging.

2. Materials and Methods

2.1. Contrast agents

Three commercially available contrast agents: iohexol (240 mg/ml or 1.89 mmol/ml, Omnipaque™, GE Healthcare), gadobutrol (605 mg/ml or 1 mmol/ml, Gd-BT-DO3A, Gadavist™, Bayer HealthCare Pharmaceuticals Inc.), gadobenate dimeglumine (529 mg/ml or 0.5 mmol/ml, Gd-BOPTA, Multihance™, Bracco Diagnostics Inc.), were compared in the study for clinical relevance. Gd-BT-DO3A and Gd-BOPTA are widely used in clinics as MRI contrast agents, but they have different gadolinium concentrations and molecular structures. Thus, both of these agents were used to help better understand how Gd contrast agents perform as CT contrast agents. Each contrast agent was diluted with phosphate buffered saline (PBS) to 1/32, 1/64, 1/128, 1/256 and 1/512 of the original concentration. The dilutions are intended to cover the large range of iodine concentration expected in various clinical situations, from high iodine concentration in the arterial phase imaging such as for pulmonary embolus scans to relatively low concentrations as expected for venous phase imaging of the liver. The samples were then placed in six rows of a 96-well plate with duplicate rows for each contrast agent. Additional wells contained PBS.

2.2. Imaging technique and image analyses

The diluted contrast solutions were scanned in a 96-well plate placed on top of a CT water phantom (20 cm diameter x 23 cm height) for additional attenuation and put on the patient table (Fig. 1). Scanning was performed in triplicate using routine clinical abdominal-pelvic protocols on two dual-energy scanners, DSCT (Siemens SOMATOM Force, Siemens Healthcare AG, Erlangen, Germany) and DLCT (Philips Spectral CT 7500, Philips Healthcare, Eindhoven, Netherlands). Routine clinical scanning protocols were used for clinical relevance. The clinical scanning parameters used in these routine protocols are different for the DSCT and the DLCT scanners. On the DSCT, 100/Sn150 kV, 105/55 mAs (6.30 mGy), rotation time of 0.5 s and pitch of 0.6 were used. On the DLCT, 120 kV, 313 mAs (20 mGy), rotation time of 0.5 s and pitch of 1.15 were used. 40, 50, 60, 70 and 80 keV VMIs were reconstructed using the manufacturer-suggested method for each scanner. The 50-50 mix of low and high energy images (standard manufacturer algorithm) were used as the conventional reconstruction on the DSCT scanner, and 120 kV conventional (standard manufacturer algorithm) images were separately reconstructed on the DLCT scanner. For DSCT scanner, iterative reconstruction ADMIRE (Advanced Modeled Iterative Reconstruction) level of 3 was used. For the DLCT scanner, iDose[4] level of 3 and spectral level of 4 were used. ADMIRE and iDose4 are CT manufacturers' proprietary iterative reconstruction algorithms. The levels represent the strength of image noise reduction, with higher numbers indicating stronger noise reduction. Images were analyzed on 2-mm coronal slices since the 96-well plate was placed on a horizontal plane. The mean HU and its standard deviation (SD) were measured with 9-mm^2 ROIs in Siemens Syngo Via (Siemens Healthcare AG, Erlangen, Germany) and in Philips IntelliSpace Portal (Philips Healthcare, Eindhoven, Netherlands).

Table 1
Mean HU of iohexol, Gd-BOPTA, and Gd-BT-DO3A with 1/32, 1/64, 1/128, 1/256, and 1/512 dilutions in conventional reconstructions as well as 70- and 80-keV images. Note that the HUs from conventional scans are similar to 70 keV for DLCT but to 80 keV for DSCT.

DSCT									
	Iohexol			Gd-BOPTA			Gd-BT-DO3A		
	70 keV	80 keV	Conv. Recon	70 keV	80 keV	Conv. Recon	70 keV	80 keV	Conv. Recon
1/32 dilution	1485	1133	1154	624	506	522	817	662	684
1/64 dilution	882	672	680	360	286	293	424	341	352
1/128 dilution	463	352	356	191	150	157	214	172	178
1/256 dilution	238	179	183	98	75	81	106	83	89
1/512 dilution	122	91	95	57	42	47	59	45	51

DLCT									
	Iohexol			Gd-BOPTA			Gd-BT-DO3A		
	70 keV	80 keV	Conv. Recon	70 keV	80 keV	Conv. Recon	70 keV	80 keV	Conv. Recon
1/32 dilution	1018	753	1085	376	316	412	551	463	598
1/64 dilution	549	403	594	229	192	254	289	243	319
1/128 dilution	289	211	321	107	88	121	126	104	142
1/256 dilution	130	91	150	42	33	49	51	42	59
1/512 dilution	49	30	59	11	8	15	11	7	15

2.3. Statistical analyses

Mean standard deviation of SD measurements (e.g., 2 samples x 3 scans = 6 SD measurements) was used as the noise estimate. SNR was calculated using the mean standard deviation as the noise estimate ($SNR = \frac{mean}{mean\ standard\ deviation}$). Wilcoxon matched-pairs signed-
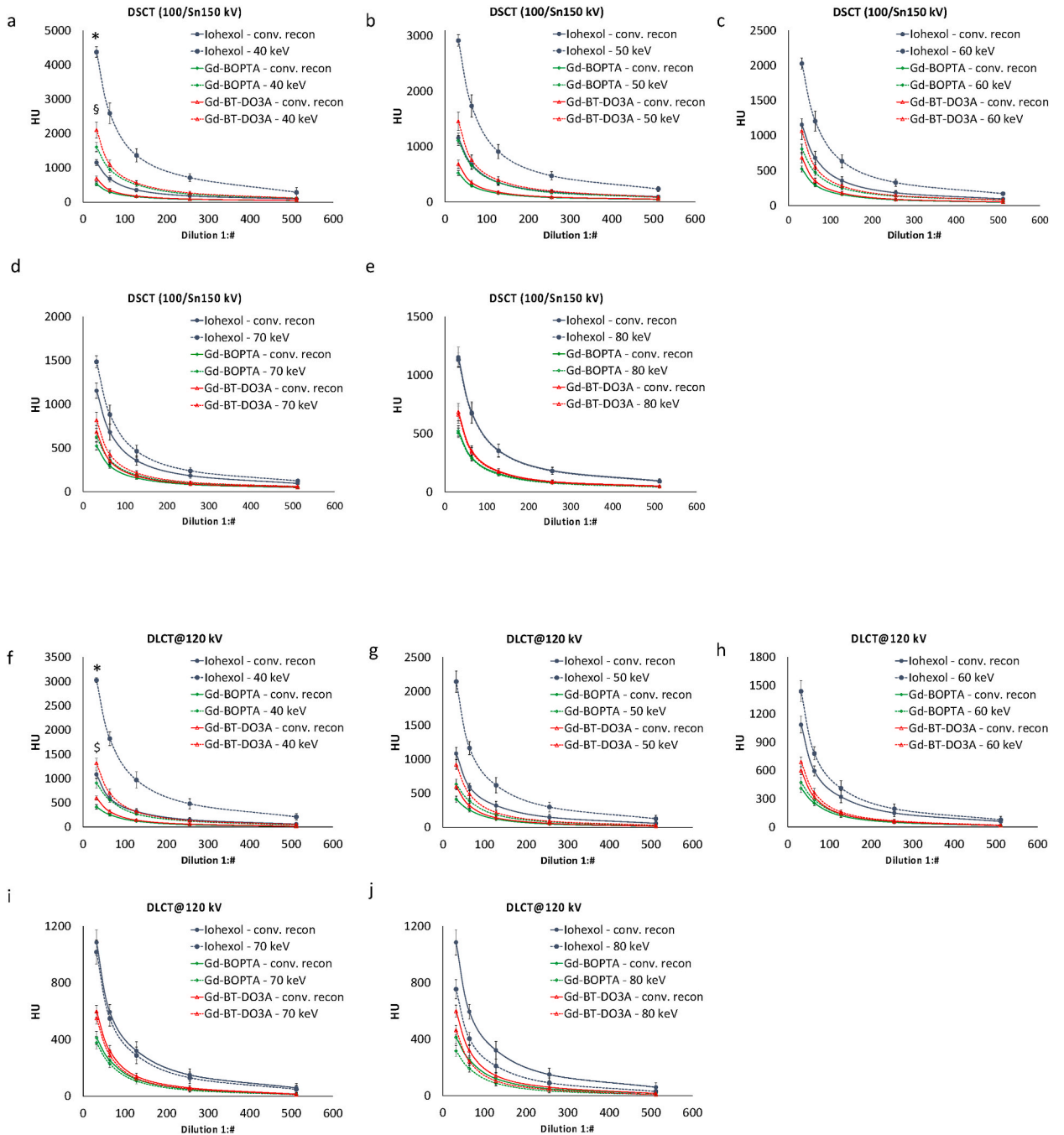

Fig. 3. HU of iohexol, Gd-BOPTA and Gd-BT-DO3A versus concentrations at conventional polyenergetic reconstruction and 40 keV monoenergy reconstruction. HU of iohexol, Gd-BOPTA and Gd-BT-DO3A versus concentrations with conventioual polyenergetic and 40 keV monoenergy reconstructions on a dual source CT (a, b, c, d, and e) and a dual-layer CT (f, g, h, i, and j). *, p < 00.05 in comparisons between HU of iohexol at 40 keV and its conventional reconstruction with both scanner types; §, p < 00.05, Gd-BOPTA/Gd-BT-DO3A @ 40 keV and iohexol with conventional reconstruction with DSCT; and $, p < 0.05, Gd-BT-DO3A @ 40 and iohexol with conventional reconstruction with DLCT (no significant difference between Gd-BOPTA and iohexol with conventional reconstruction). DSCT: dual-source dual energy CT; DLCT: dual-layer dual energy CT. Dilution 1: # means that the value on the x-axis represents the ratio 1:x or 1/x. For instance, x = 32 represents a 1/32 dilution.
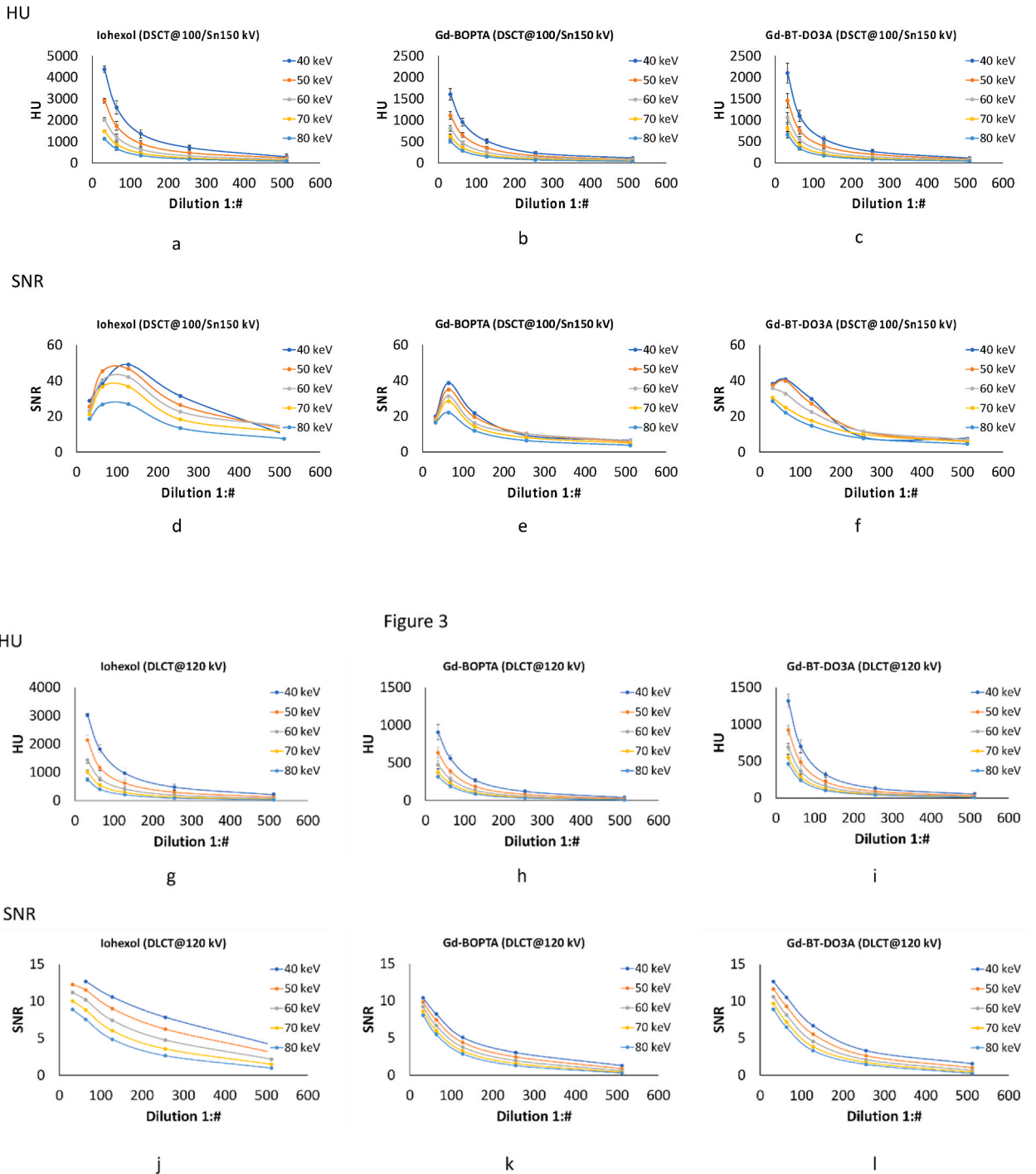
HU

SNR

Figure 3

HU

SNR

Fig. 4. HU and SNR of monoenergy reconstructions at various contrast dilutions. HU (a, b, c; g, h, i) and SNR (d, e, f; j, k, l) of iohexol, Gd-BOPTA and Gd-BT-DO3A versus concentrations at 40, 50, 60, 70 and 80 keV monoenergy on a dual source CT (a, b, c, d, e and f) and a dual-layer CT (h, i, j, k, l and m). SNR for 1/32 dilution at 40 keV in (j) excluded due to saturation. DSCT: dual-source dual energy CT; DLCT: dual-layer dual energy CT. Dilution 1:# means that the value on the x-axis represents the ratio 1:x or 1/x. For instance, x = 32 represents a 1/32 dilution.
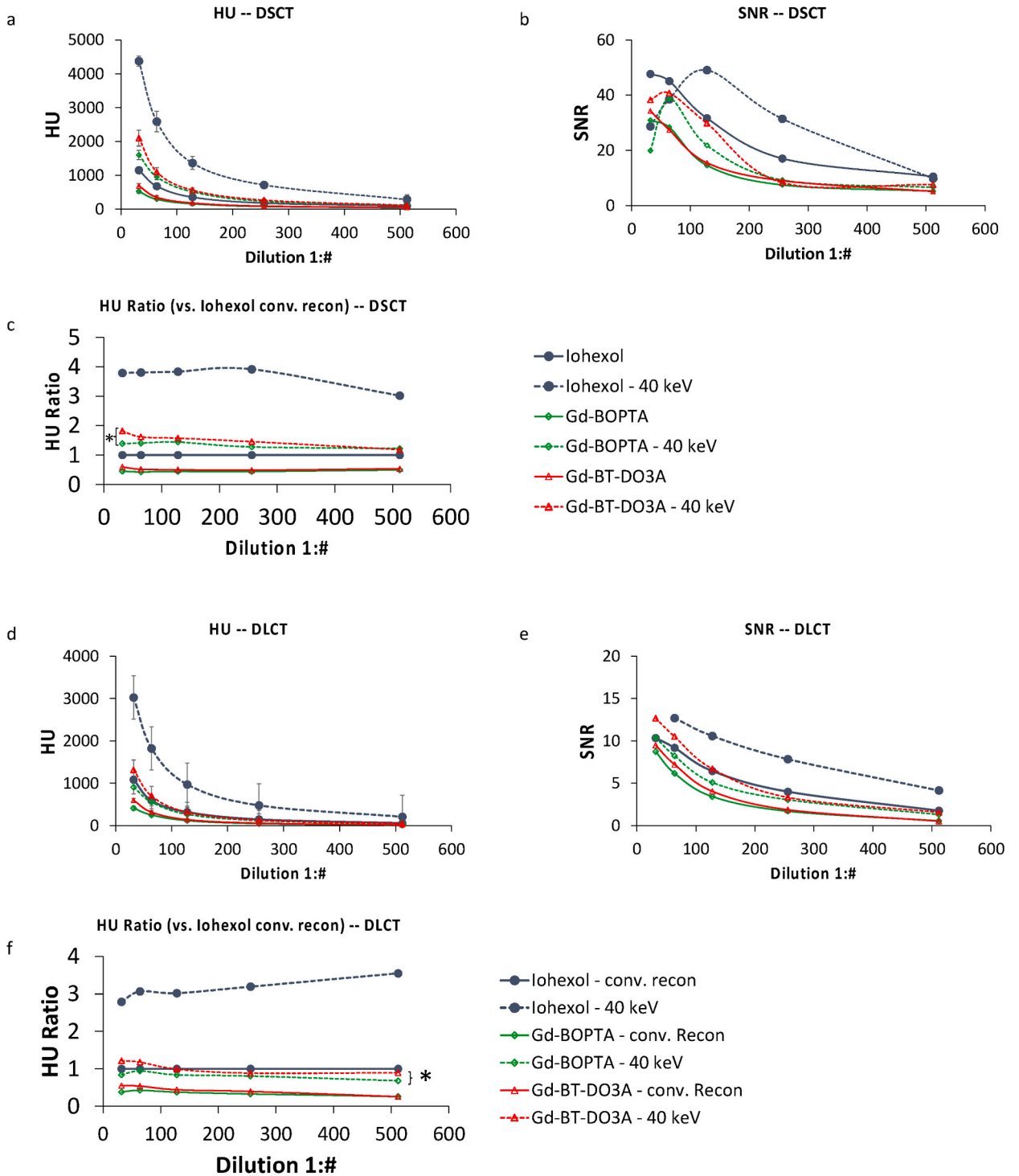
Fig. 5. HU, SNR and HU ratio of I and Gd-based contrast agents compared to iohexol with conventional polyenergy reconstruction. HU (a) and SNR (b) of conventional polyenergy and 40-keV monoenergy reconstructions at various contrast concentrations. HU ratio of contrast agents compared to iohexol with conventional polyenergetic reconstruction (c) at various contrast concentrations on a dual source CT (a, b, c) and a dual-layer CT (d, e, f). SNR for 1/32 dilution at 40 keV in (e) excluded due to saturation. *, p < 0.001, HU ratio for Gd-BT-DO3A significantly greater than that of Gd-BOPTA with both scanners. DSCT: dual-source dual energy CT; DLCT: dual-layer dual energy CT. Dilution 1:# means that the value on the x-axis represents the ratio 1:x or 1/x. For instance, x = 32 represents a 1/32 dilution.

rank test in Stata/SE 15.1 (StataCorp LLC. College Station, TX) [19] was used to compare HU between two different keV levels on the same scanner and Wilcoxon rank-sum test was used to compare HU of different contrast agents.

3. Results

HUs of different dilutions of each agent were plotted at various keV levels whereas the HUs from conventional scans were plotted as isobars for DSCT and DLCT (Fig. 2). For iodinated- and Gd-based agents, these intersected at approximately 70 keV for DLCT compared to approximately 80 keV for DSCT (Fig. 2, indicated by arrow; Table 1). For all agents, HU increased inversely with keV and at lower keV were greater than conventional (at 40 keV, $p < 0.0001$). For the iodine-based contrast agent, the highest HUs were at 40 keV for both scanners, near the k-edge of iodine of 33 keV. Similar results were seen with the Gd agents although the k-edge of Gd is 50 keV. 40 KeV showed significantly greater HU than 50 Kev for all agents ($p < 0.05$).

Fig. 3a–e are plots of HU against dilution levels at each keV level on DSCT, and Fig. 3f–j are the same plots on DLCT. HU of Gd-based agents with DSCT at 50 keV was similar to iodine-based agent with conventional (Fig. 3b) whereas 40 keV was similar with DLCT (Fig. 3f). Further, Gd-based agents had greater HUs at 40 keV than the iodine-based agent with conventional on DSCT (Fig. 3a, $p < 0.05$). Comparing the two Gd-based agents, at lower keVs and greater concentrations (less dilute), HU of Gd-BOPTA was less than that of Gd-BT-DO3A ($p < 0.05$) on both scanners.

Between scanners, DSCT HUs were greater than DLCT HUs at 40 keV; further, DLCT HUs at 40 keV were similar to DSCT at 50 keV (Fig. 3b and f). Overall, the HU values for the DSCT scanner appeared to be shifted to the right by 10 keV compared to DLCT (i.e., DSCT HU values at 50 keV were similar to DLCT at 40 keV, 60 keV to 50 keV, etc).

For both iodine- and Gd-based agents, SNR generally increased inversely with keV (Fig. 4d–f and j-l), like HU (Fig. 4a–c and g-i). On both scanners, the SNRs of both the iodine- and Gd-based agents were generally similar. However, on the DSCT, SNR peaked at the second or third dilution for the iodine-based agent, second for Gd-BOPTA and first or second dilution for Gd-BT-DO3A; whereas, SNR decreased monotonically with contrast concentrations with conventional reconstruction (Fig. 4d–f, 5b). In contrast, SNR monotonically decreased with concentration in both VMIs and conventional images on the DLCT (Fig. 4j-l and 5e).

Fig. 5a and b are plots of HU against dilution levels of conventional reconstruction images and 40-keV VMIs for all three contrast agents on the DSCT and DLCT, respectively. Fig. 5c and d show the ratio of HU in Fig. 5a and b to the HU of iohexol in the conventional images at each dilution level. Approximately 3-fold (median for all samples) increase in HU was noted at 40 keV compared to conventional reconstruction with iodine-based contrast for the DLCT and approximately 4-fold (median for all samples) for the DSCT ($p > 0.9$ when comparing medians at various dilution levels); i.e., 1/3 to 1/4 concentration of the iodine contrast agent is detectable at 40 keV compared to conventional reconstruction.

Comparing the Gd-based agents with iodine-based, taking the ratio (Fig. 5c–f) at each dilution, for the DLCT, HU of the Gd-based agents at 40 keV are similar to those of the iodine-based with conventional reconstruction, whereas, it is approximately 1.5 fold greater using the DSCT ($p > 0.3$ when comparing medians at various dilution levels). This HU ratio trend is greater for Gd-BT-DO3A versus Gd-BOPTA with both scanners ($p < 0.001$).

4. Discussion

We used two types of DECT scanners and compared image contrast at clinically relevant keVs with an iodine-based and two Gd-based contrast agents. Iodine- and Gd-based contrast HU increased inversely with respect to keV for the same dilution. At the lowest keV setting of 40 keV, the iodine-based contrast agent HU with the DLCT and DSCT were approximately 300 % and 400 % of that with conventional reconstruction, respectively. Gd-based contrast agent HU in VMIs from 40 keV were similar to iodine-based contrast HU using conventional reconstructions. Furthermore, similarity of HUs in VMIs with conventional reconstruction are scanner-dependent, with 70 keV noted for a DLCT and 80 keV for a DSCT scanner. When comparing the DSCT and DLCT, both iodine- and Gd-based agent HU in VMIs for the DSCT appear to be shifted to the right by 10 keV compared to the DLCT.

Three-fold iodine-based contrast HU increase in DLCT VMIs and four-fold in DSCT VMIs with 40-keV compared to conventional reconstruction indicates that it may be possible to use 1/4 to 1/3 of the full clinical dose while maintaining similar HU. This finding is supported by a Gd-BT-DO3A phantom study with a Siemens DSCT [20]. This is significantly lower than the 7/10th reduction that has been used empirically with conventional reconstructions during the recent IV contrast shortage and 50 % iodinated-contrast dose reduction that has been purported using DLCT at low keV [21]. The shape of the HU curves for the Gd-based contrast agents mimicked those based on iodine. A recent study using DSCT [22] suggests that the VMI at 50 keV provides better contrast enhancement for a Gd-based agent, but lower keV was not discussed. Our study suggests that 40 keV further improves enhancement of both iodine- and Gd-based contrast.

VMI HU was scanner type dependent. In terms of iodine- and gadolinium-based contrast HU, overall the entire keV curve evaluated (40–80 keV) using the DLCT appeared to be shifted by 10 keV to the right compared to DLCT. Findings suggest that scanner-dependent protocol optimization and potentially calibration are needed.

In terms of Gd-based contrast safety, although one study suggested nephrotoxicity with high doses of a Gd agent in a porcine model with conventional CT [23,24], such reports are lacking clinically including with new Gd-agents with greater binding constants. With the advent of macrocyclic and newer linear MR contrast agents, nephrogenic systemic fibrosis that may be associated with intravenous MR contrast agents has essentially disappeared [25]. Although gadolinium-based contrast agent deposition has been reported such as in the brain and bones, no clear evidence of clinical consequences associated with gadolinium retention has been established [26–28].

Although the mass attenuation of Gd is 50 % higher than I due to the better match of its 50-keV k-edge to typical 100–140 kV used

in CT, a typical iodine-based contrast agent has three iodine atoms per molecule in distinction to one Gd atom per molecule for a typical Gd-based contrast agents [29]. However, with 40 keV VMI, clinically feasible Gd-based contrast agent volumes (doses) should be feasible, particularly for more concentrated contrast agent applications such as arterial imaging. This is supported by our findings and suggested by clinical studies [30]. Remy-Jardin M et al. found that ~50 ml of 0.5 mmol/L Gd chelate provided adequate enhancement in pulmonary angiography using conventional multidetector CT [31]. Approximately 3 fold enhancement at 40 keV compared to conventional acquisition noted in our study suggests ~18 ml would be adequate using 40 keV VMI. In an 11 patients coronary CTA study at 40 keV [26], 0.2 mmol/kg was used implying 14 ml at 1 mmol/ml for a 70 kg man. These volumes are within ~1–2 doses of standard MR doses used clinically and double doses have been used for MR angiography. Thus, Gd-based agents have the potential to serve as alternatives to iodine-based agents for DECT depending on the clinical application.

Despite lower HU with the Gd-based agents than iohexol, the SNRs were similar for Gd- and I- based agents at various dilutions, indicating their image quality is similar in terms of SNR. Furthermore, SNR and HU generally increased inversely with keV and the effect trended greater with less dilution (more concentrated) of I- or Gd-based contrast. The findings also support that Gd-based agents may be more effective alternatives in procedures with high contrast concentration in targets. These findings are supported by other studies with Gd-BT-DO3A on a DSCT scanner [20,22].

Given Gd k-edge of 50 keV, peak HU was expected at 50 keV for the Gd-based agents if the k-edge effect was detected. However, HU did not decrease at 40 keV, indicating apparently these iodine-oriented VMI algorithms cannot detect the k-edge effect of Gd; practically, this suggests 40 keV should be preferred for greater HU, hence image contrast.

This study has limitations. First, this study did not perform image metrics for other aspects of image quality such as spatial resolution and noise texture, but rather focused on HU and SNR. Although some studies indicate spatial resolution is similar among various keV levels [32–34], noise texture at 40 keV is different from that at 70 or 80 keV [32], suggesting possible differences in lesion detectability. However, 40-keV images can be used as complementary images alongside conventional reconstructions, providing better image contrast information. Second, routine clinical acquisition protocols for each scanner were used for clinical relevance, thus neither noise nor radiation dose are matched on the two scanners limiting comparison of SNR between scanners, but this should not affect conventional scan HU measurements, which are calibrated routinely. The conventional images on the DSCT do not come from a conventional 120-kV acquisition rather are an equal-weighted mix of low and high kV images acquired with the 100/150Sn kV setting as suggested by the manufacturer and routinely used in our clinic. Comparison between the conventional CT reconstruction on DLCT and DSCT may be biased since the DLCT used only 120-kV acquisitions as suggested by the manufacturer and routinely used in our clinic.

In summary, compared to conventional reconstruction, 40-keV VMI allowed for similar HU with approximately 1/3-1/4 of the concentration of iodinated intravenous contrast, suggesting potentially substantial dose reductions with DECTs. Additionally, HU in VMIs varies by scanner type, suggesting scanner-dependent protocol optimization and potentially VMI HU calibration are needed. At similar dilutions, Gd-based contrast agents at 40 keV provide similar or greater HU than conventional reconstruction with iodinated contrast. Therefore, with appropriated selection of Gd-contrast agent and scanners, Gd-based contrast agents could potentially serve as alternatives to Iodine-based ones for 40 keV VMI for select clinical applications.

Data availability statement

Data will be made available on request.

CRediT authorship contribution statement

Guang Li: Writing – review & editing, Writing – original draft, Visualization, Validation, Supervision, Software, Project administration, Methodology, Investigation, Formal analysis, Data curation. **Nikita Rednam:** Writing – review & editing, Methodology, Investigation, Data curation. **Vikas Kundra:** Writing – review & editing, Writing – original draft, Visualization, Validation, Supervision, Resources, Project administration, Methodology, Investigation, Funding acquisition, Formal analysis, Data curation, Conceptualization.

Declaration of competing interest

References

[1] H.S. Gurm, S.R. Dixon, D.E. Smith, et al., Renal function-based contrast dosing to define safe limits of radiographic contrast media in patients undergoing percutaneous coronary interventions, J. Am. Coll. Cardiol. 58 (9) (2011) 907–914.
[2] O. Toprak, M. Cirit, Risk factors for contrast-induced nephropathy, Kidney Blood Press. Res. 29 (2) (2006) 84–93.

[3] M.R. Rudnick, A.K. Leonberg-Yoo, H.I. Litt, et al., The controversy of contrast-induced nephropathy with intravenous contrast: what is the risk? Am. J. Kidney Dis. 75 (1) (2020) 105–113.

[4] T.S. Ahuja, N. Niaz, M. Agraharkar, Contrast-induced nephrotoxicity in renal allograft recipients, Clin. Nephrol. 54 (1) (2000) 11–14.

[5] H.S. Thomsen, T. Almen, S.K. Morcos, Contrast Media Safety Committee Of The European Society Of Urogenital R, Gadolinium-containing contrast media for radiographic examinations: a position paper, Eur. Radiol. 12 (10) (2002) 2600–2605.

[6] S.P. Lin, J.J. Brown, MR contrast agents: physical and pharmacologic basics, J Magn Reson Imaging 25 (5) (2007) 884–899.

[7] S. Sudarski, P. Apfaltrer, J.W. Nance Jr., et al., Optimization of keV-settings in abdominal and lower extremity dual-source dual-energy CT angiography determined with virtual monoenergetic imaging, Eur. J. Radiol. 82 (10) (2013) e574–e581.

[8] K. Matsumoto, M. Jinzaki, Y. Tanami, et al., Virtual monochromatic spectral imaging with fast kilovoltage switching: improved image quality as compared with that obtained with conventional 120-kVp CT, Radiology 259 (1) (2011) 257–262.

[9] H.N. Cardinal, D.W. Holdsworth, M. Drangova, et al., Experimental and theoretical x-ray imaging performance comparison of iodine and lanthanide contrast agents, Med. Phys. 20 (1) (1993) 15–31.

[10] K.L. Grant, T.G. Flohr, B. Krauss, et al., Assessment of an advanced image-based technique to calculate virtual monoenergetic computed tomographic images from a dual-energy examination to improve contrast-to-noise ratio in examinations using iodinated contrast media, Invest. Radiol. 49 (9) (2014) 586–592.

[11] N. Rassouli, M. Etesami, A. Dhanantwari, P. Rajiah, Detector-based spectral CT with a novel dual-layer technology: principles and applications, Insights Imaging 8 (6) (2017) 589–598.

[12] J.R. Wortman, J.W. Uyeda, U.P. Fulwadhva, A.D. Sodickson, Dual-energy CT for abdominal and pelvic trauma, Radiographics 38 (2) (2018) 586–602.

[13] D.E. Morgan, The role of dual-energy computed tomography in assessment of abdominal oncology and beyond, Radiol. Clin. 56 (4) (2018) 565–585.

[14] T. D'Angelo, G. Cicero, S. Mazziotti, et al., Dual energy computed tomography virtual monoenergetic imaging: technique and clinical applications, Br. J. Radiol. 92 (1098) (2019) 20180546.

[15] M.H. Albrecht, T.J. Vogl, S.S. Martin, et al., Review of clinical applications for virtual monoenergetic dual-energy CT, Radiology 293 (2) (2019) 260–271.

[16] A. Gupta, E.G. Kikano, K. Bera, et al., Dual energy imaging in cardiothoracic pathologies: a primer for radiologists and clinicians, Eur J Radiol Open 8 (2021) 100324.

[17] M.M. Obmann, G. Punjabi, V.C. Obmann, et al., Dual-energy CT of acute bowel ischemia, Abdom Radiol (NY). 47 (5) (2022) 1660–1683.

[18] W. Kazimierczak, N. Kazimierczak, A. Lemanowicz, et al., Improved detection of endoleaks in virtual monoenergetic images in dual-energy CT angiography following EVAR, Acad. Radiol. 30 (12) (2023) 2813–2824.

[19] StataCorp, Stata Statistical Software: Release 15, StataCorp LLC, College Station, TX, 2017.

[20] M.N. Bongers, C. Schabel, B. Krauss, et al., Potential of gadolinium as contrast material in second generation dual energy computed tomography - an ex vivo phantom study, Clin. Imag. 43 (2017) 74–79.

[21] Y. Nagayama, T. Nakaura, S. Oda, et al., Dual-layer DECT for multiphasic hepatic CT with 50 percent iodine load: a matched-pair comparison with a 120 kVp protocol, Eur. Radiol. 28 (4) (2018) 1719–1730.

[22] S.J. Nogel, L. Ren, L. Yu, et al., Feasibility of dual-energy computed tomography imaging of gadolinium-based contrast agents and its application in computed tomography cystography: an exploratory study to assess an alternative option when iodinated contrast agents are contraindicated, J. Comput. Assist. Tomogr. 45 (5) (2021) 691–695.

[23] B. Elmstahl, U. Nyman, P. Leander, et al., Gadolinium contrast media are more nephrotoxic than a low osmolar iodine medium employing doses with equal X-ray attenuation in renal arteriography: an experimental study in pigs, Acad. Radiol. 11 (11) (2004) 1219–1228.

[24] B. Elmstahl, U. Nyman, P. Leander, et al., Gadolinium contrast media are more nephrotoxic than iodine media. The importance of osmolality in direct renal artery injections, Eur. Radiol. 16 (12) (2006) 2712–2720.

[25] M. Mathur, J.R. Jones, J.C. Weinreb, Gadolinium deposition and nephrogenic systemic fibrosis: a radiologist's primer, Radiographics 40 (1) (2020) 153–162.

[26] Administration FaD, FDA Drug Safety Communication: FDA Identifies No Harmful Effects to Date with Brain Retention of Gadolinium-Based Contrast Agents for MRIs; Review to Continue, 2017.

[27] V. Gulani, F. Calamante, F.G. Shellock, et al., Gadolinium deposition in the brain: summary of evidence and recommendations, Lancet Neurol. 16 (7) (2017) 564–570.

[28] N. Iyad, S.A. M, S.G. Alkhatib, M. Hjouj, Gadolinium contrast agents- challenges and opportunities of a multidisciplinary approach: literature review, Eur J Radiol Open 11 (2023) 100503.

[29] D.S. Gierada, K.T. Bae, Gadolinium as a CT contrast agent: assessment in a porcine model, Radiology 210 (3) (1999) 829–834.

[30] J. Nadjiri, D. Pfeiffer, A.S. Straeter, et al., Spectral computed tomography angiography with a gadolinium-based contrast agent: first clinical imaging results in cardiovascular applications, J. Thorac. Imag. 33 (4) (2018) 246–253.

[31] M. Remy-Jardin, J. Bahepar, J.J. Lafitte, et al., Multi-detector row CT angiography of pulmonary circulation with gadolinium-based contrast agents: prospective evaluation in 60 patients, Radiology 238 (3) (2006) 1022–1035.

[32] S. Suzuki, R. Fukui, S. Harashima, W. Samejima, Effect of energy level on the spatial resolution and noise frequency characteristics of virtual monochromatic images: a phantom experiment using four types of CT scanners, Jpn. J. Radiol. 40 (1) (2022) 94–102.

[33] O. Ozguner, A. Dhanantwari, S. Halliburton, et al., Objective image characterization of a spectral CT scanner with dual-layer detector, Phys. Med. Biol. 63 (2) (2018) 025027.

[34] F. van Ommen, E. Bennink, A. Vlassenbroek, et al., Image quality of conventional images of dual-layer SPECTRAL CT: a phantom study, Med. Phys. 45 (7) (2018) 3031–3042.